

Torque Boost Operation of New Consequent-Pole Permanent Magnet Motor Using Zero-Phase Circuit

Toshihiko Noguchi
Graduate School of Integrated
Science and Technology
Shizuoka University
Hamamatsu, Japan
noguchi.toshihiko@shizuoka.ac.jp

Kazuhiro Murakami
Graduate School of Integrated
Science and Technology
Shizuoka University
Hamamatsu, Japan
murakami.kazuhiro.14a@shizuoka.ac.jp

Akihisa Hattori
DENSO CORPORATION
Kariya, Japan
akihisa.hattori.j6p@jp.denso.com

Yoichi Kaneko
DENSO CORPORATION
Kariya, Japan
yoichi.kaneko.j6y@jp.denso.com

Abstract—A novel consequent-pole permanent magnet (PM) motor is proposed in the paper, which has image pole pairs for every pole pair of N and S. The three-phase synchronous impedances of the motor are balanced owing to the rotor configuration. In addition, it is possible to carry out field weakening with less d-axis current, which leads to a highly efficient operation in a high-speed range. However the motor still has a drawback of low torque generation at low speeds due to less PM volume. In order to solve the problem, the paper discusses a torque boost operation by introducing a zero-phase winding to the motor and a three-phase four-wire motor drive circuit with an inverter. This paper describes a basic principle of the newly proposed consequent-pole PM motor and its operation characteristics, and investigates the torque boost approach using the proposed system.

Keywords—consequent-pole permanent magnet motor, field weakening operation, zero-phase current, torque boost

I. INTRODUCTION

Research and development aiming at operation range enlargement of the permanent magnet (PM) motors are intensively promoted in recent years. The PM motor can be designed so as to generate a higher torque in a low-speed range by increasing the electromotive force (e.m.f.) with high-energy-density PMs such as NdFeB and SmCo. In principle, however, it is impossible to design the PM motor to achieve both of the high-speed operation and the high-torque generation at low-speeds at the same time; hence field weakening techniques are widely introduced to suppress the e.m.f. in the high-speed operation range.

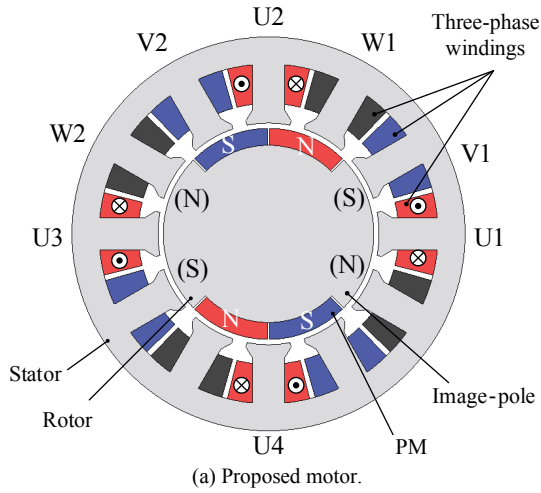
Since the field weakening operation is generally carried out by injecting a negative d-axis current to cancel the PM magnetic flux and the e.m.f. generation, the copper loss due to the d-axis current is unavoidable in the high-speed region, which degrades efficiency of the PM motor. Therefore, it is strongly required to develop a novel configuration of the PM motor that can achieve efficient field weakening with less d-axis current. In order to make it possible to reduce the d-axis current, a novel geometry of the PM motor that can increase the d-axis inductance is indispensable because more counter magnetic flux against the PM magnetic flux can be easily generated with the less d-axis current.

In this paper, a novel consequent-pole PM motor is proposed, which has a unique alignment of the PMs rather different from a conventional consequent-pole PM motor. The proposed PM motor has an image pole pair per one pair of N and S real PM poles on the rotor. There are two important features about the proposed motor, i.e., the three-phase synchronous impedances are balanced, and the d-axis inductance is increased. Therefore, torque ripple can be effectively suppressed, and the field weakening operation is efficiently carried out with the less d-axis current. Both of the above advantages make it possible to expand the whole operation range and to improve the operation efficiency.

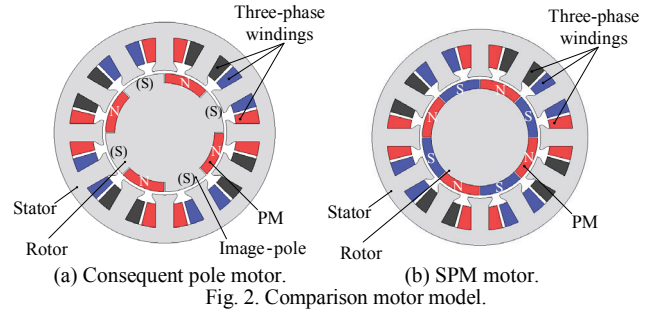
However, it is rather difficult to avoid low-torque generation in the low-speed range because of lack of the PM volume inherently caused by the consequent pole configuration. In order to solve this problem, a composite magnetomotive force (m.m.f.) of the proposed consequent pole PM motor has been focused on to improve the torque generation characteristics in the low-speed range. In the paper, basic operation characteristics of the proposed consequent pole PM motor are discussed, compared with a standard surface PM (SPM) motor and a conventional consequent pole PM motor. In addition, an approach to boost the output torque in the low-speed range is presented, utilizing a zero-phase current as well as normal three-phase currents, which can be achieved by taking advantage of the composite m.m.f. of the proposed motor.

II. CONFIGURATION AND OPERATING PRINCIPLE

Figure 1 shows a cross section of the proposed consequent pole PM motor. The motor employs equivalent eight-poles (four real PM poles and four image poles) and 12-slot concentrated winding structure, which contributes to the downsizing of the motor. The real PM pole pairs are mounted on the rotor and the image pole pairs are formed between the real PM pole pairs. This configuration is rather different from conventional consequent pole PM motors, and this unique configuration gives the following advantages. Focusing on the U-phase winding, for example, two teeth of the twelve are always facing with the real PM pole pairs, while the other two teeth are always on the image pole pairs, i.e., iron core parts. This feature is same in the V-phase and the W-phase, which



(a) Proposed motor.
(b) Winding structure of proposed motor.
Fig. 1. Proposed motor model.



(a) Consequent pole motor. (b) SPM motor.
Fig. 2. Comparison motor model.

TABLE I. MOTOR SPECIFICATIONS.

	Proposed PM motor	Consequent pole PM motor	SPM motor
Stator diameter	80 mm	←	←
Rotor diameter	42.85 mm	←	←
Stack length	37 mm	←	←
Air gap length	1.045 mm	←	←
Number of poles	8 (PM:4, Image pole:4)	8 (PM:4, Image pole:4)	8
Number of slots	12	←	←
Number of turns	16	←	←
PM volume	7.672 cc	7.672 cc	15.344 cc
Armature winding connection	4-series star connection	←	←
PM type	NMX-43SH	←	←

cannot be expected in the conventional consequent pole PM motors. Therefore, the magnetic circuit of the rotor iron core is necessarily imbalance, but the impedance of the stator windings can be balanced if the two windings on the real PM pole sides and the other two windings on the image pole sides are connected in series. The three-phase balanced windings do not affect on the motor current control in spite of the imbalance rotor magnetic circuit and give the freedom of magnetic circuit design of the image pole pair parts on the rotor.

The proposed motor has a high inductance value because it has lower magnetic flux due to the half amount of the PM and the higher amount of the rotor iron than standard SPM motors. The e.m.f. of the motor is expressed as (1)

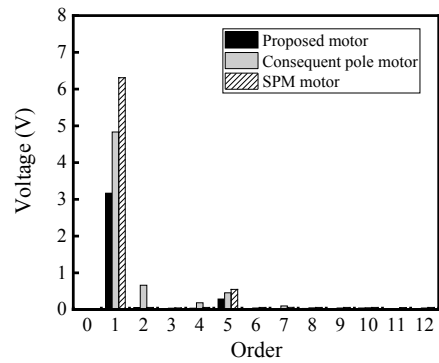
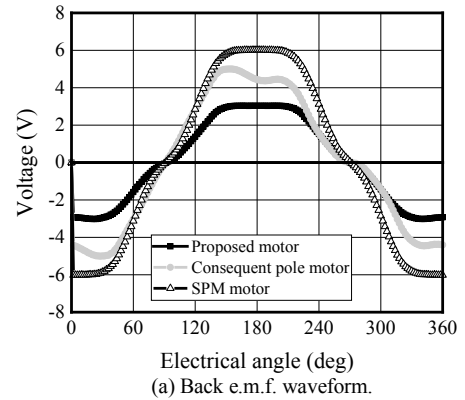
Therefore, the electromagnetic torque of the motor is lower in a low-speed range, but the efficient high-speed operation can be expected because it requires reduced negative d-axis current owing to the lower magnetic flux of the field PM and the higher inductance value of the stator windings.

$$V_0 = \omega \sqrt{(\Psi_a + L_d i_d)^2 + (L_q i_q)^2} \quad (1)$$

III. OPERATION CHARACTERISTICS OF PROPOSED MOTOR

A. Comparison of No-Load Electromotive Force

Comparison of the operation characteristics has been made among the proposed motor, a conventional consequent pole PM motor, and a standard surface PM (SPM) motor, using an electromagnetic analysis software JMAG-Designer 18.0TM. The proposed motor model is indicated in Fig. 1, and the other motor models are in Fig. 2, of which detailed specifications are listed in TABLE I. The motor volume of all the three



(a) Back e.m.f. waveform.
(b) FFT result.
Fig. 3. Comparison of back e.m.f. and FFT analysis results.

motors is identical, whereas only the rotor geometries of the three are different from each other. The proposed motor and the conventional consequent pole motor have equivalent eight poles on the rotor (four real PM poles and four image poles composed with iron core), but the standard SPM motor has eight real PM poles; hence the PM volume is double of the consequent pole PM motors.

Figure 3 shows the no-load e.m.f. waveforms of the U-phase and their FFT analysis results when the three motors are operated at 600 r/min. The e.m.f. amplitude of the proposed motor is almost half of that of the SPM motor because the PM volume is 50 % of the SPM motor's. Therefore, the proposed motor can extend the high-speed operation range. The proposed motor has a lower e.m.f. constant and more fundamental component in the e.m.f. waveform, compared with the conventional consequent pole PM motor: thus the motor is suitable for the high-speed operation with field weakening control.

B. Comparison of Inductance

Figure 4 shows variations of the d-axis and the q-axis inductances of the three models, where the current phase angle β is changed under the constant stator current amplitude. As the β increases, the d-axis inductance as well as the q-axis inductance is increased because the amounts of the magnetic fluxes to the both axes are reduced.

The d-axis inductance of the proposed motor is the highest among the three motors, and is larger by approximately 45 % than the SPM motor, which means that the reluctance of the magnetic circuit in the proposed motor is the least. The SPM motor has the minimum inductance values in both of the d-axis and the q-axis. However, the conventional consequent pole PM motor has the highest q-axis inductance. As described above, any types of the consequent pole PM motors have more iron in the rotor cores and higher inductance values, compared with the standard SPM motor of which rotor is entirely surrounded by the PMs. As can be expected, the proposed motor is capable to realize the field weakening with less d-axis current owing to the higher d-axis inductance.

C. Harmonics Comparison of Magnetic Flux

Harmonic components of the magnetic flux has been compared among the three motors. Only the d-axis current of 20 A is given to the motor, where the electromagnetic analysis has been conducted under an assumption of the ideal iron rotor using the PMs replaced with air. Figure 5 shows the magnetic flux linkages of the U-phase and their FFT analysis results of the three motors. Because the permeance variation is hardly caused in the SPM motor, only the fundamental component is seen in the FFT result. On the other hand, the conventional consequent pole PM motor has a significant permeance variation due to the real PM poles and the image poles on the rotor, resulting in the even-order harmonic components of the magnetic flux linkage. However, the proposed motor is not affected by the permeance variation because one U-phase winding is facing with the real PM pole while the other U-phase winding is on the image pole side; hence the even-order harmonic components are not seen in the magnetic flux linkage to the U-phase winding.

D. Comparison of N-T Characteristics

N-T characteristics of the three motors are indicated in Fig. 6, where the maximum output power is delivered to the loads. The test conditions are 12-V DC bus voltage, the maximum

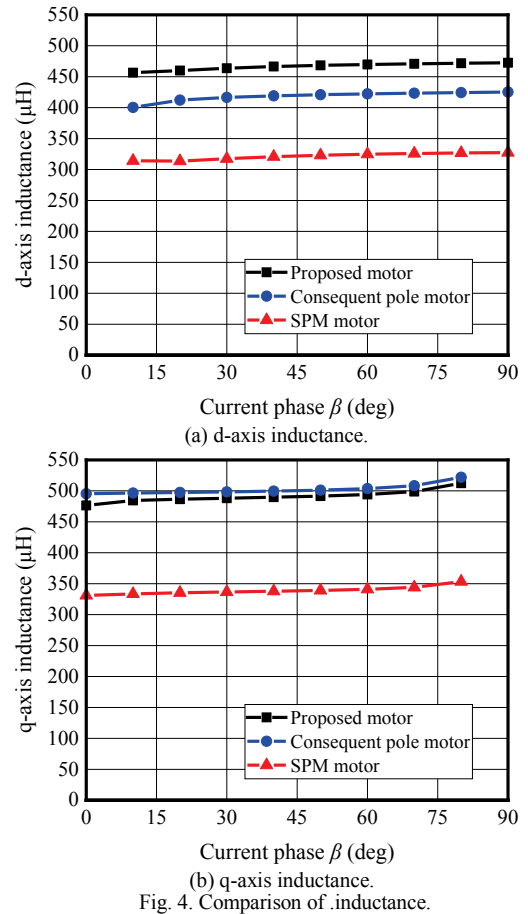


Fig. 4. Comparison of inductance.

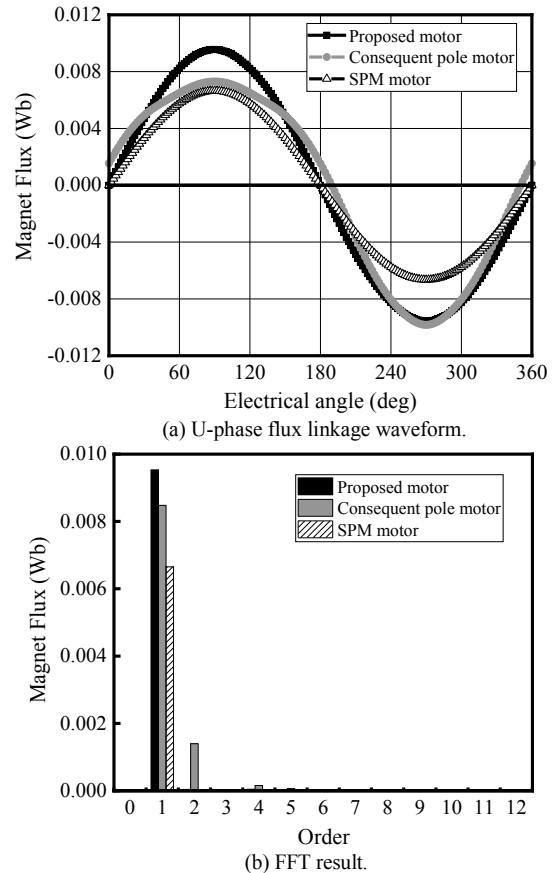


Fig. 5. Comparison of U-phase flux linkage.

current amplitude of 20 A, and the maximum m.m.f. of 1280 AT.

The SPM motor can deliver the higher torque in the low-speed range owing to the high e.m.f., compared with the other motors. On the other hand, the proposed motor can expand the higher-speed range because the motor has a low-coefficient of the e.m.f. and the counter e.m.f. is high enough to cancel the PMs' e.m.f. Therefore, the higher-speed range can effectively be expanded by means of the field weakening. The conventional consequent pole PM motor has almost same N-T characteristic as the SPM motor, and is hard to expand the high-speed operation range. This is due to the even-order harmonic components in the e.m.f. when the field weakening is applied to the motor.

As described above, it has been found that the proposed motor has the largest high-speed operation range with the least negative d-axis current; thus the field weakening operation can efficiently be achieved among the three motors.

IV. COMPOSITE MAGNETOMOTIVE FORCE OF PROPOSED MOTOR

As described in the previous section, the proposed consequent pole PM motor can expand the high-speed operation range with the less field weakening current, i.e., the negative d-axis current. It is difficult, however, to obtain the higher torque in the low speed range because the e.m.f. coefficient is almost half of that of the standard SPM motor. As mentioned previously, the PM amount of the SPM motor is exactly twice of the proposed motor, so it is necessary to consider enhancement of the torque generation without sacrificing the wide-speed operation range of the proposed motor.

The conventional standard SPM motor has the space m.m.f. distribution of the PMs that synchronizes a rotating magnetic field generated by the stator three-phase windings. In other words, the m.m.f. of the rotor has only the positive sequence component with less harmonic components. However, the proposed motor has not only the eight-pole component but also the four-pole component of the rotor m.m.f. Figure 7 illustrates a composite m.m.f. of the proposed motor. As can be seen in the figure, it is possible to decompose the proposed consequent poles (four real PM poles and four image poles) to a set of the two full PM m.m.f. distributions, i.e., one is a four-pole m.m.f. distribution, and the other is an eight-pole m.m.f. distribution.

If the proposed motor has two sets of the three-phase stator windings, i.e., the four-pole windings and the eight-pole windings, it is possible to generate higher torque by feeding these windings with two inverters. One inverter must be operated synchronously with the eight-pole m.m.f. component, and the other inverter must drive the motor synchronously with the four-pole m.m.f. component. In the case, the combined operation of the two inverters is indispensable, and six-wire connection to the two inverters is necessary, which is a drawback of the motor drive utilizing the composite m.m.f.

Therefore, the novel motor drive technique is investigated in the paper, where the proposed motor with the composite m.m.f. can be driven by a single inverter. Figure 8 shows a cross section of the proposed consequent pole PM motor with double stator windings, i.e., one set of the windings is a normal three-phase windings, and the other is a special single-phase winding. The three-phase windings synchronize with the

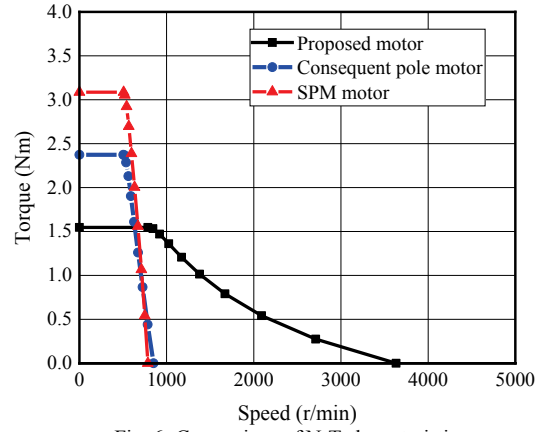


Fig. 6. Comparison of N-T characteristics.

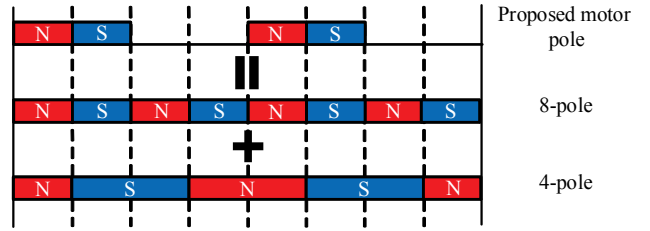


Fig. 7. Illustration of proposed motor magnet arrangement.

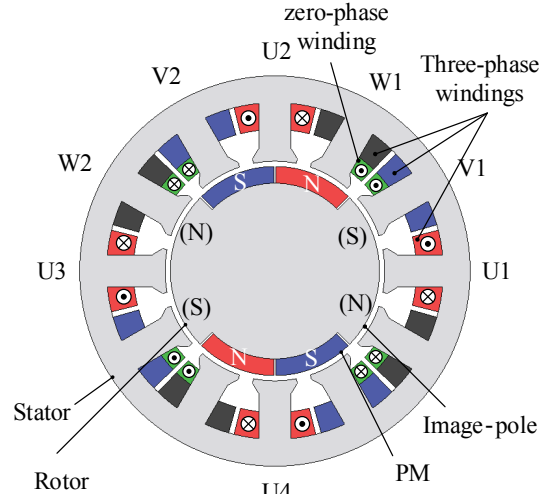


Fig. 8. Proposed motor with double stator winding model.

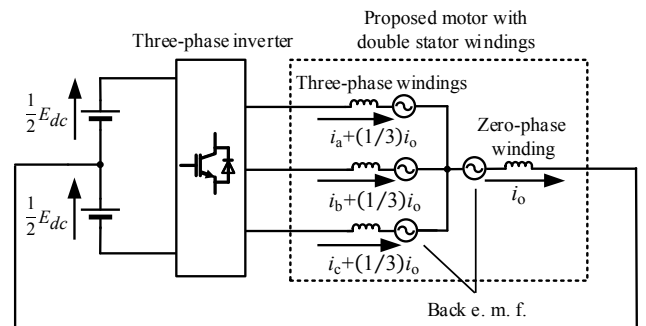


Fig. 9. Motor drive circuit using zero-phase winding.

eight-pole m.m.f. component, while the single-phase winding generates additional torque with the four-pole m.m.f. component. Figure 9 shows a circuit configuration of the motor drive with a single inverter. As shown in the figure, the single-phase winding is connected to the neutral point of the three-phase windings and the midpoint of the inverter DC bus. Therefore, the current flowing into the single-phase winding can independently be controlled at a different amplitude, a different frequency, and a different phase angle from those of the three-phase windings, using the common mode (zero-phase) current in the circuit. An alternating magnetic field is generated by the single-phase winding and the zero-phase current, and is synchronized with the four-pole m.m.f. of the rotor, which is easily carried out by superimposing the single-phase AC onto the three-phase currents. The drawback of the proposed approach is a large torque ripple caused by the alternating magnetic field generated by single-phase winding and the single-phase common mode current. However, it is possible to generate additional torque with no extra three-phase inverters.

V. OPERATION CHARACTERISTICS EXAMINED THROUGH SIMULATIONS

A. Magnetomotive Force of Proposed Motor

Operation characteristics have been examined through computer simulations using an electromagnetic analysis software JMAG-Designer 18.0TM. The motor model and its specifications are shown in Fig. 8 and TABLE II, respectively. Figure 10 is the rotor surface magnetic flux density distribution and its FFT analysis result of the proposed motor. It is confirmed that the motor has two sets of the real PM pole pairs and that there are two parts with no magnetic flux density corresponding to the iron core parts. In addition, both of the four-pole component and the eight-pole component can be confirmed in the FFT analysis of the magnetic flux density distribution, which demonstrates the composite m.m.f. of the rotor.

B. No-Load Electromotive Force

No-load e.m.f. of the three-phase windings and the other no-load e.m.f. of the single-phase winding are depicted in Fig. 11 and Fig. 12, respectively. These e.m.f. waveforms and their FFT analysis results are measured at the rotating speed of 600 r/min. As can be seen in these figures, the three-phase e.m.f. waveforms are almost sinusoidal because they do not contain low-order harmonic components. On the other hand, the e.m.f. waveform of the single-phase winding is close to rectangular because it contains odd-order harmonic components of which amplitudes are approximately inverse proportional to the orders. The frequency of the three-phase e.m.f. is 40 Hz, which corresponds to the eighth-order (eight poles) component, while the single-phase e.m.f. frequency is 20 Hz, which is fourth-order (four poles) component.

C. Torque Boost Operation

Therefore, three-phase sinusoidal currents to the three-phase windings can generate smooth torque without the torque ripple in principle, and a single-phase rectangular current to the single-phase winding can generate additional average torque with torque ripple. As described previously, independent current control is possible in the three-phase windings and the single-phase winding owing to the three-phase four-wire motor drive circuit configuration with an inverter. The rectangular currents with 1/3 amplitude of the single-phase winding is superimposed to the three-phase

TABLE II. MOTOR SPECIFICATIONS.

	Proposed motor with double stator windings
Stator diameter	80 mm
Rotor diameter	42.85 mm
Stack length	37 mm
Air gap length	1.045 mm
Number of poles	8 (PM:4, Image pole:4)
Number of slots	12
Number of zero-phase turns	10
Number of three-phase turns	16
PM volume	7.672 cc
Three-phase winding connection	4 series
Zero-phase winding connection	4 series
PM type	NMX-43SH

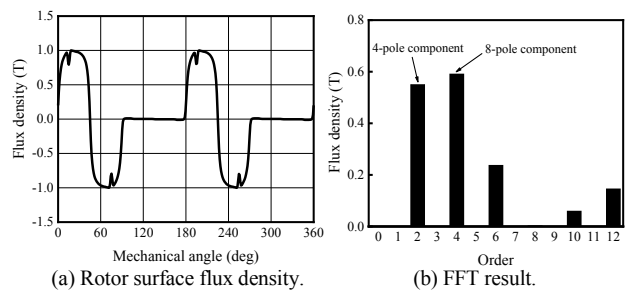


Fig. 10. Rotor surface flux density and FFT analysis result.

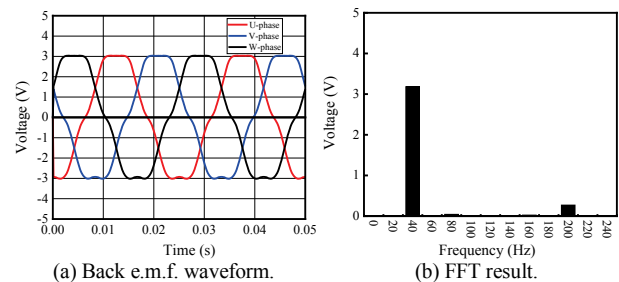


Fig. 11. Back e.m.f. waveforms and FFT analysis result of proposed motor three-phase windings.

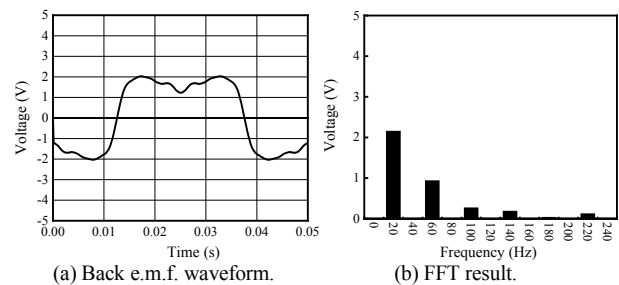


Fig. 12. Back e.m.f. waveforms and FFT analysis result of proposed motor zero-phase winding.

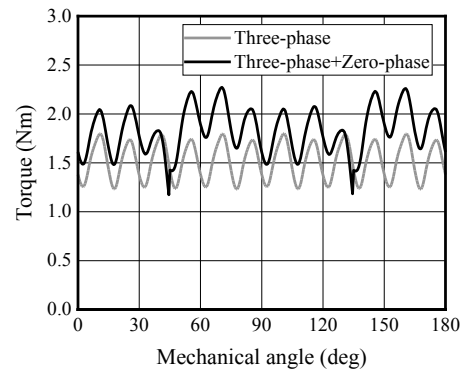
currents. The simulation test conditions are 20-Arms rectangular current, which generates $800 A_{rms}T$ m.m.f. in the single-phase winding, while the $1280 A_{rms}T$ m.m.f. is given to the three-phase windings, respectively. Figure 13 shows torque waveforms and their FFT analysis results when the proposed motor is driven by only the three-phase windings and when the motor is driven by both of the three-phase windings and the single-phase winding. Although the proposed method generates low-even-order harmonic torque components, it can boost the average torque by 20 %. These even-order harmonics in the torque waveform is caused by the alternating magnetic field generated by the single-phase winding and the zero-phase current, but the extra average torque is effectively added to the torque delivered by the normal three-phase windings.

VI. CONCLUSION

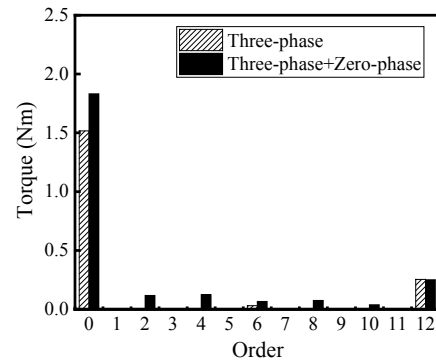
A novel consequent pole PM motor has been proposed, and its operating characteristics have also been investigated in the paper. The proposed motor has a unique rotor configuration where the real PM pole pairs and the image pole pairs are placed every other pole pair. The image pole pairs are constituted on the iron core parts next to the real surface PMs on the rotor. one of the most important features of the proposed motor is high-speed operation capability with less field weakening current (negative d-axis current); thus efficient expansion of the high-speed operation range is possible without increasing copper loss.

In addition to the above basic operation characteristics, the paper has proposed torque boost operation. Focusing on the composite m.m.f. of the proposed motor, a four-pole and an eight-pole synchronous rotating magnetic fields are generated in the motor at the same time. Therefore, it is possible to boost the torque by utilizing both magnetic fields. In order to achieve the torque boost operation, a four-pole single winding is added to the normal three-phase windings in the motor. By introducing a three-phase four-wire motor drive circuit configuration with a single inverter, it has been confirmed that the average torque can be effectively increased by the single phase winding.

In the future work, influence of the e.m.f. generated in the additional single-phase winding must be investigated because the potential variation at the neutral point of the three-phase windings may affect the voltage margin of the inverter. It is also required to investigate the mutual interference between the three-phase windings and the single-phase winding and to design the stator iron core that has an independent slot configuration.



(a) Torque waveforms.



(b) FFT results.

Fig. 13. Torque waveforms and FFT analysis results between three-phase and three-phase plus zero-phase.

REFERENCES

- [1] H. Hijikata, K. Akatsu, "A Study of Dual Winding Method for Compound Magnetomotive Force Motor" IEEJ Trans. Industrial Applications. Vol. 133, No. 10, pp. 986-994, 2013.
- [2] K. Akatsu, and S. Wakui, "A Design Method of Fractional-slot Concentrated Winding SPMSM Using Winding factor and Inductance factor", IEEJ Trans. Industrial Applications. Vol. 127, No. 11, pp. 1171-1179, 2007.
- [3] T.A. Lipo and M. Aydin, "Field Weakening of Permanent Magnet Machines - Design Approaches", Power Electronics and Motion Control Conference, Riga, Latvia, 2004.
- [4] S. Morimoto, Y. Takeda, T. Hirasa, K. Taniguchi, "Expansion of Operating Limits for Permanent Magnet Motor by Current Vector Control Considering Inverter Capacity", IEEE Trans. on Industry Applications, IA-26, No. 5, pp. 866-871, 1990.
- [5] S. Morimoto, K. Hatanaka, Y. Tong, Y. Takeda, T. Hirasa, "Variable Speed Drive System of Permanent Magnet Synchronous Motors with Flux-weakening Control", IEEJ Trans. Industrial Applications. Vol. 112, No. 3, pp. 292-298, 1992.
- [6] U. Ekong, M. Inamori, and M. Morimoto "Field-Weakening Control for Torque and Efficiency Optimization of a Four-Switch Three-Phase Inverter-Fed Induction Motor Drive," IEEJ J. Industry Applications, Vol. 8, No. 3, pp. 548-555, 2019.
- [7] J. A. Tapia, F. Leonardi, T. Lipo: "Consequent-Pole Permanent Magnet Machine with Field Weakening Capability", Proc. of IEMDC 2001, pp. 126-131, 2001.
- [8] T. Ogawa, T. Takahashi, M. Takemoto, S. Ogasawara, H. Arita, and A. Daikoku "Increasing the Operating Speed of a Consequent Pole Axial Gap Motor for Higher Output Power Density," IEEJ J. Industry Applications, Vol. 8, No. 3, pp. 497-504, 2019.